



Universiteit
Leiden
The Netherlands

The evolving velocity field around protostars

Brinch, C.

Citation

Brinch, C. (2008, October 22). *The evolving velocity field around protostars*. Retrieved from <https://hdl.handle.net/1887/13155>

Version: Corrected Publisher's Version

License: [Licence agreement concerning inclusion of doctoral thesis in the Institutional Repository of the University of Leiden](#)

Downloaded from: <https://hdl.handle.net/1887/13155>

Note: To cite this publication please use the final published version (if applicable).

Chapter 1

Introduction

1.1 The birth of stars

On a clear, dark night it is possible to make out a faint nebulosity with the unaided eye in the constellation of Orion. This is the Orion Nebula, part of the giant Orion Molecular Cloud, and it is a vast reservoir of cold molecular gas and interstellar dust. Although the Orion Nebula is the only molecular cloud visible to the naked eye, similar clouds are numerous scattered throughout the Milky Way and some of them are close enough to Earth, so that they can be studied in great detail using telescopes. Stars are known to form inside these clouds and therefore molecular clouds have been the subject of intense study during the last 30 years, in the pursuit of a complete understanding of the various processes leading from the relatively simple cloud material into a solar-type star, complete with a planetary system, moons, comets and possibly biology.

While the conceptual outline of what is known as low-mass ($\leq 1M_{\odot}$) star formation is generally well understood, almost every detail about how the initial conditions, i.e. the chemo-physical properties of the local cloud environment, are reflected in the emerging star and planets, if any, are not. At present it is not known why some stars form as doubles or even multiples while others do not. It is also not known why some stars are found to have planetary systems while others seem to have none. There is no doubt that the variation found in stars and their planetary systems are somehow linked to the variation in the molecular clouds out of which they formed. However, it is an open question whether the dependence is predictable or whether the end product of star formation is governed by random (and unpredictable) external effects.

The development of the theory of low-mass star formation began more than 30 years ago. In the early days, the formation of a star was described by an inside-out collapse of a spherical cloud (Shu 1977). As the cloud gets gravitationally unstable, gas and dust start to fall toward the center reaching free-fall speed



Figure 1.1: The star forming region NGC1333 on the edge of the Taurus Molecular Cloud as imaged by the Spitzer Space Telescope at infrared wavelengths. (NASA/JPL-Caltech/R. A. Gutermuth (Harvard-Smithsonian CfA))

and the collapse front expands outward with the local sound speed. This theory, known as the Shu collapse, was not able to treat angular momentum however, as it was spherical symmetric in nature, and therefore no stellar rotation, binary star systems, or disks could be formed. Throughout the 1980's, the collapse theory of Shu was modified to include angular momentum in a series of papers (e.g., Cassen & Moosman 1981; Bodenheimer 1981; Terebey et al. 1984; Lin & Pringle 1990). During the same period, observational evidence for rotational motions in the parental cloud cores were found (Benson & Myers 1989; Goodman et al. 1993) and it became clear that this rotation would lead to the formation of a disk as the centrifugal force would break the spherical symmetry. Eventually, all the cloud material ends up in either the star or the disk (disregarding winds and jets which are still not well understood), which would now be in stable Keplerian rotation. At present, no analytical model exists which can reproduce this entire scenario, but numerical simulations have been successful in producing disks out of collapsing rotating clouds (e.g., Boss 1993; Burkert et al. 1997; Yorke & Bodenheimer 1999).

On the observational side, young stellar objects were found to have different

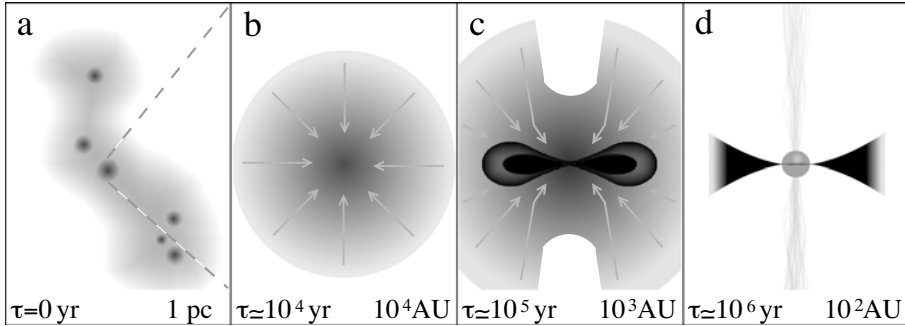


Figure 1.2: A cartoon depiction of the stages of low-mass star formation. **a)** An inhomogeneous molecular cloud with several overdense regions, so called cloud cores. **b)** A cloud core is triggered into gravitational collapse when it reaches its Jeans mass. Material moves radially toward the center of the core under the influence of gravity. **c)** Due to turbulence and shear motions of the molecular cloud, the core has a net angular momentum which makes the material spin up as the core contracts. The result is a rotating disk of material onto which material is accreted from the still collapsing molecular envelope. **d)** A T Tauri star emerges when all of the envelope has either been accreted or blown away by the bipolar outflow that characterizes these objects. The remaining material is located in a protoplanetary disk.

spectral energy distributions. Indeed, Lada & Wilking (1984) showed that the slope of the distribution between $10 \mu\text{m}$ and $20 \mu\text{m}$ would divide a sample of protostars into two distinct categories giving rise to the Class I/II/III classification scheme. Later on, a Class 0 was added by André et al. (1993) for protostars with a strong far-infrared excess. The interpretation of this classification is that the more infrared excess a star shows, the more embedded in dust it is. Class 0 stars are therefore thought to be deeply embedded protostars, shown as panel b in Fig. 1.2, the Class I stars less embedded (panel c, Fig. 1.2), and Class II stars unobscured T Tauri stars as shown in panel d, Fig. 1.2. As suggested by Fig. 1.2, these classes represent a linear time evolution, going from Class 0 to Class II over time. Whether this is really true or not and whether all stellar spectral energy distributions will appear in all three classes over time is not clear. It is also not well-understood if these classes really represent physically distinct populations or whether there is an overlap.

The long time scales on which star formation takes place ($> 10^6$ years) make

it impossible to follow a single star through the various stages of the formation process. Indeed, in almost all circumstances, any given young star will be seen as a snapshot representing its present evolutionary stage, even throughout the entire life of an astronomer. However, by observing a number of young stars on different evolutionary stages, a chronological sequence can be pieced together. If young stars can be placed reliably in an evolutionary sequence, various physical properties, such as dust grain sizes, chemical abundances, etc., can be followed in time and the influence of the cloud environment can be followed throughout the entire star formation process.

The challenging part is to disentangle evolutionary differences between a number of objects from intrinsic differences because of the degeneracies between the two. An example of this is the stellar mass. One could think of using the stellar mass as tracer of evolution, assuming that the mass of the star grows during its formation. In that case a more massive star would be considered a more evolved star than a less massive one. However, stars end up with a wide range in masses and therefore the more massive star could simply be an intrinsically more massive star at the same evolutionary stage as one which is intrinsically less massive.

Consequently, a lot of research in the field of low-mass star formation is concerned with finding reliable tracers of evolution (basically a tracer of the age of an object, although the time scale is almost certainly an object dependent variable itself). Attempts are made to use the ongoing chemistry as a tracer of evolution. Charnley et al. (1992) have suggested to use abundance ratios, whereas Jørgensen et al. (2004) use the abundance profiles, as a “chemical clock”. Various attempts are also made to constrain the classification scheme of Lada & Wilking (1984) with better time-scale estimates (e.g., Adams et al. 1987; André & Montmerle 1994; Allen et al. 2004; Luhman et al. 2008). This thesis revolves around the topic of low-mass protostellar evolution with special emphasis on the feasibility of using the gas kinematics as a tracer of evolution.

1.2 The study of molecular emission lines

The gas-phase molecular material which is present in protostellar environments is the main diagnostic tool used in this thesis. It is typically observed in the (sub)millimeter regime of the electromagnetic spectrum, because the conditions of the circum-(proto)stellar environment are such that material located there will radiate at those frequencies (10-1000 GHz). In particular, we study emission associated with rotational transitions since the rotational bands are dominant at temperatures between 10 and 100 K, typical for the gas surrounding protostars. We

study molecular line emission rather than thermal continuum radiation, associated with the dust grains, because the motion of the gas is directly reflected in the line position through the velocity induced Doppler shift. Hence, by studying emission lines, we can derive information about the velocity field around protostars.

1.2.1 Line formation

Line emission is the result of spontaneous or induced de-excitation of a molecule according to the famous relation

$$h\nu = E_1 - E_2. \quad (1.1)$$

The energy eigenstates E_i are molecule dependent and the allowed transitions between states are described by selection rules, resulting in a unique set of possible photon frequencies for each molecular species. The reverse process, excitation of energy states, depends on the physical environment, in particular the temperature and density, which thus controls the relative population of the energy levels E_i . The emergence of a line spectrum occurs when the photons from an ensemble of molecules, which are being continuously excited and de-excited, are measured over a period of time.

Although Eq. 1.1 suggests that the transition occurs at a single well-defined frequency, every transition in general results in a spread of the emission over a range of frequencies. Several mechanisms can cause this so-called line broadening, of which the most fundamental is called natural line broadening. This effect is due to the quantum mechanical uncertainty relation that allows variation in the transition energy given a sufficiently well-defined period of time. For rotational transitions, this effect is small however, compared to the Doppler broadening which is a temperature dependent effect. The motion of the molecule relative to the observer causes a Doppler shift of the line center, proportional to the velocity difference between the molecule and the observer. In a gas consisting of many molecules, the velocities are given by a Maxwellian velocity distribution resulting in a continuous line center shift over the corresponding velocities. When adding the contribution of all molecules along the line of sight, this results in a continuous Gaussian line profile.

Under interstellar conditions, where temperatures typically are relatively low (< 100 K), the thermal Doppler broadening has a small effect on the spectral line width (~ 0.1 km s⁻¹ for CO at 10 K). If however, a systematic velocity field is present in the emitting medium, a non-thermal Doppler broadening occurs, which can be substantial. The exact shape of the resulting line profile depends on the

composition of the velocity field and it is this effect that we rely on, when we characterize the motion of the circumstellar material using spectral line profiles. Figure 1.3 shows an illustration of how different line profiles result from different velocity fields. The figure shows a protostellar envelope with an inner region with a high excitation temperature and an outer region with a low excitation temperature. The velocity vectors show the direction of the flow as well as the projected line-of-sight velocity. Two dashed ovals are also plotted in the figure. These ovals are loci of constant projected velocity, so that at the two points where the line-of-sight intersects these loci the projected velocity is the same. The bulk of the emission originates from the high excitation temperature region. This is true for both the red-shifted and blue-shifted side. In the infall case (panel a), however, only the red-shifted emission passes through the locus intersection in the low excitation temperature region, where part of the emission is absorbed. In the case of pure rotation (panel b), the red-shifted and blue-shifted sides are equally absorbed.

1.2.2 Modeling of line profiles

When observing an emission line of interstellar origin, the line will in most cases originate from a large number of molecules (i.e., a cloud of gas) which is distributed over a range in densities and temperature. Moreover, the distribution is in general not homogenous, resulting in a variation of the relative abundance over the region being studied. This makes forward solving of the physical structure of the cloud impossible. Instead, a physical model is adopted and the radiation field escaping the model cloud is predicted, from which a model line spectrum can be calculated. This line model can then be compared to the measured line, and in case of a good match, the adopted model is likely to give a good description of the cloud.

In a cloud of gas, a photon emitted from a decaying state of one molecule can either escape the cloud and contribute to the emission line or, depending on the optical depth, excite the same state of another molecule on its way toward the cloud surface. In the latter case, the newly excited molecule decays after a while and the photon is reemitted in a random direction and can possibly excite another molecule again. The more molecules that exist in the excited state, the smaller the chance of the photon getting absorbed on its way out. However, the chance of a radiative de-excitation is increased, which will thus lower the number of excited molecules and increase the number of absorptions again.

This coupled dependency between the radiation field and the level excitation makes the problem of predicting the emerging emission line difficult and it needs to be solved iteratively. The emission and absorption probabilities does not just

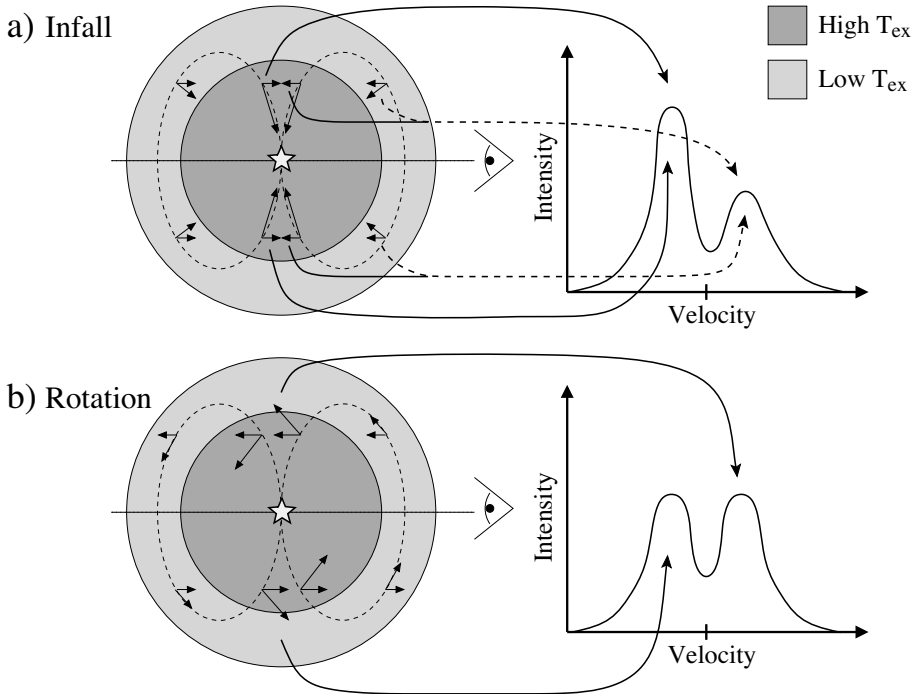


Figure 1.3: A schematic depiction of the influence of the velocity field in a gaseous envelope on the line profile. The dashed ovals are loci of constant projected velocity. Any line of sight will intersect these loci at two different excitation temperatures T_{ex} . In panel **a)**, blue-shifted emission from the high T_{ex} region travels unobscured toward the observer, while red-shifted emission from the high T_{ex} region is obscured by the material with the same velocity in the low T_{ex} region. In panel **b)**, both the red and the blue sides are equally affected. Figure inspired by Zhou & Evans (1994).

depend on the level populations, but also on the local temperature and density which adds to the complexity of the computational task. Furthermore, the velocity field, which causes a Doppler shift of the photons, ensures that only molecules with a small relative velocity can interact through an exchange of photons. Obviously, this cannot be solved analytically except for the simplest cases and therefore radiation transfer codes are employed to make predictions of the emission lines. In this thesis we make extensive use of one such code, known as *RATTRAN* (Hogerheijde & van der Tak 2000), but we have also developed our own code, which we

present in a later chapter.

In order to reach a match between the observed lines and the lines predicted by the model, several adjustable parameters are included. Most of these can be constrained by other observables than emission lines; for example, the temperature and density profiles are fixed from measurements of the dust continuum brightness profiles at different frequencies. The velocity field however, is only constrainable through comparison of spectral lines, because these are the only observables which directly reflect the velocity of the emitting medium. Throughout this thesis we use a two dimensional parameterization of the velocity field,

$$\mathbf{v} = \begin{pmatrix} v_r \\ v_\phi \end{pmatrix} = \sqrt{\frac{GM_*}{r}} \begin{pmatrix} -\sqrt{2} \sin \alpha \\ \cos \alpha \end{pmatrix}, \quad (1.2)$$

where the two free parameters M_* and α represent the protostellar mass and the ratio of infall speed to rotation speed, respectively. These two numbers describe the velocity field and, as we show in a later chapter, they can be used to characterize the evolutionary state of a protostellar object. This parameterization gives us a smooth transition from pure infall to pure rotation and we can therefore use it to determine when an object is dominated by one or the other.

1.2.3 Submillimeter observations

Our primary diagnostic tool is formed by the emission lines associated with rotational transitions of various molecular species and these bands lie in the radio wave part of the electromagnetic spectrum. Radio telescopes are used to measure these frequencies and in this thesis, we use a variety of such observations.

As with all telescopes, the spatial resolution of radio wave observations is proportional to the wavelength and inversely proportional to the telescope dish diameter. Because radio waves lie in the low-frequency (long wavelength) domain of the electromagnetic spectrum, the telescopes have to be huge in order to reach a decent angular resolution. However, the dish surface smoothness has to be of the order of a fraction of the wavelength, which, for submillimeter observations, therefore requires very smooth surfaces. One of the biggest telescopes that fulfill this criterion is the James Clerk Maxwell Telescope in Hawaii with a mirror diameter of 15 meters. This telescope is able to observe most low- J rotational transitions between 0.5 mm and 1.0 mm at a resolution of $10''$ – $20''$, depending on the wavelength. At this resolution, young stellar objects, at a typical distance of the order of 100 pc, are only marginally resolved if resolved at all. The fact that the sources are not well resolved, however, can be useful to us in some cases.

Because our velocity model (Eq. 1.2) has no spatial dependency, it is suited to fit observations where the velocity field has been spatially averaged in a large beam that covers the entire object. Studying objects in more detail, however, require observations of much higher resolution and this is needed when we investigate the velocity field on disk scales.

In order to achieve higher resolution we need to do interferometric observations rather than the more traditional single-dish observations. The technique is to link several telescopes together and letting the signal from each antenna interfere with the signal from each of the other antennas, while measuring the phase and amplitude of the interference. Interferometry becomes increasingly difficult going toward higher frequencies because the wavelength becomes small and hence better timing accuracy is needed. In the last ten years several millimeter interferometry facilities have become operational around the world, but, only one of them, the Submillimeter Array in Hawaii, operates at shorter wavelengths than 1mm. For this thesis, interferometric data have been obtained from the Submillimeter Array. Images can be reconstructed with a resolution that is an order of magnitude higher than the best obtainable single-dish resolution. With the increased resolution, we are not only able to probe the velocity field in distinct regions of an object, but we can also constrain global properties such as the shape of the gaseous envelope, system inclination, etc. The interferometric observations are very well complimented by the single-dish observations, because by using both types of observations to constrain the models simultaneously, we make sure that our model is consistent with the data on all probed spatial scales.

1.3 Thesis outline

A comprehensive study of the young stellar object L1489 IRS is presented in **chapter 2**. In this chapter we introduce several of the tools and techniques which we employ throughout this thesis. We take a physical model from the literature of L1489 IRS, which we customize so that we can accommodate observational features such as the envelope geometry and we introduce a parameterized description of the velocity field. The reason why we study this particular object is because of its unusual properties. First of all it has a very large size and an elongated disk-like appearance. Secondly, both infall and rotational velocity components are measured, and therefore this source is a good candidate for testing our velocity model. Our model is compared to single-dish spectra and because we have a large number of free parameters, we use a stochastic search algorithm to obtain the best fit. The minimization technique used in this chapter is based on Voronoi

tessellation of the parameter space. In **chapter 3** we use a similar, but more advanced search algorithm, whereas the Voronoi tessellation is revisited in **chapter 7**, this time as a mean of radiation transfer gridding.

Our velocity model is elaborated upon in **chapter 3**. The scope of this chapter is to evaluate general applicability of the velocity model and to test how well the best fit parameters of our model describe the actual velocity field of a particular source. A hydrodynamical simulation of the formation of a star and a circumstellar disk provides a continuous velocity field, temperature and density distribution. Synthetic observations are then calculated from our hydrodynamical solution and the velocity model which was introduced in **chapter 2** is fitted to these in a similar way as we did for L1489 IRS. We show that the best-fit parameters describe a velocity field which is in reasonable agreement with the velocity field in the simulation. In this chapter we use a genetic optimization algorithm to obtain the best fit. This algorithm proves to be very reliable and works well for our purpose.

In **chapter 4** we return to L1489 IRS, for a more detailed study. High-resolution interferometric data were acquired with the Submillimeter Array of the central, dense parts of this source. The aim of this chapter is to investigate whether it is possible to separate a possible protoplanetary disk from the envelope using kinematic arguments. We use the model derived in **chapter 2** but with the addition of a Keplerian disk model on scales smaller than 300 AU. The submillimeter data are consistent with such a model, but cannot constrain any disk properties. Simultaneous modeling of the mid-infrared fluxes from the Spitzer Space Telescope complements the submillimeter data well, however, and with these data, additional constraints strongly support the disk model.

Until this point, variations in the molecular abundance distribution have been disregarded. However, chemical depletion, which is known to exist in protostellar environments, may mask out kinematically distinct regions, in which case our velocity model gives a false result. **Chapter 5** contains a treatment of the CO depletion in the circumstellar disk and envelope. We use the same hydrodynamical simulation as used in **chapter 3** to describe the star formation and we populate the simulation with molecules that can freeze-out and desorb according to the physical environment. The resulting abundance patterns are used to calculate synthetic CO spectra. We show that the importance of taking chemical depletion into account is most important for young sources and less important for more evolved objects. Also optically thin lines are significantly more affected than their optically thick counterparts.

In **chapter 6** we employ all techniques used so far in this thesis, by modeling both single-dish and interferometric submillimeter data of the young protostel-

lar source NGC1333–IRAS2A, a source in which depletion is significant. Again we use our parameterized velocity model together with a literature model of the physical and chemical structure. Our result confirms that this is indeed a young source, by favoring a solution with a low central mass and strong infall motions (very little rotation). A particularly puzzling result is that no kinematic evidence for Keplerian rotation on 100 AU scales is found, despite the evidence for the presence of a mass condensation on these scales from the dust continuum data. This makes IRAS2A a very different kind of object, compared to L1489 IRS, from a kinematical point of view.

The last part of this thesis, **chapter 7**, is a presentation of a new radiation transfer code, based on the work of Ritzerveld & Icke (2006), which we have developed in parallel to the research presented in the previous chapters. This code is designed to improve on several shortcomings of the radiation transfer code used so far, by changing the gridding and transport algorithms fundamentally. A new gridding subroutine based on Voronoi tessellation of the model is implemented, making the code truly three dimensional, very fast, and able to resolve a much wider range of scales.

1.4 Conclusions

Several conclusions can be drawn from this thesis. We will here briefly summarize the main conclusions, not necessarily in the order in which they appear in the following chapters.

- The velocity field transits smoothly from infall to rotation during a gravitational collapse and the formation of a circumstellar disk. The velocity field can be characterized uniquely by the model parameters α and M_* .
- The mass of the protostar is highly object dependent. However, the ratio of protostellar mass to envelope mass M_*/M_{env} is likely to be the same for all low-mass stars at any given fraction of their total formation time. Along with the α parameter, this ratio traces time evolution and can be used to order objects into an evolutionary sequence.
- Depletion occurs in the envelope, especially in the early stages of the collapse. Later on depletion becomes significant in the protoplanetary disk. It is important to model depletion as it may affect the appearance of the velocity field in the spectral lines.

- If depletion is modeled properly, it may provide a way to calibrate the evolution sequence of M_* and α with an absolute time scale. This would effectively give us a kinematical clock of evolution.
- Circumstellar disks seem to form almost immediately after the initial collapse of the prestellar core. Whether or not it is reasonable to use the word disk at the very earliest point is questionable, since the rotation pattern only shows up at somewhat later stages of the collapse.
- While high-resolution observations, provided by interferometers, reveal an enormous amount of detail, it is actually preferable to combine both high and low resolution observations in order to pin down the velocity field. α is by definition an average of the ratio of infall to rotation, and the spatial averaging in the large beam of single-dish telescopes gives a good boundary condition, when fitting the velocity field.
- The geometrical properties of disks are better constrained by near-infrared imaging and mid-infrared spectroscopy due to the improved resolution and its high sensitivity to the dust column along the line of sight. While infrared continuum emission does not reveal anything about the velocity field, it can fix a number of parameters which are hard to constrain using submillimeter radiation. Furthermore, it is important that the models are consistent with the emission in all frequency bands and not just in one particular part of the spectrum.
- Often, young stellar objects are described in a very idealized way; completely spherical or axi-symmetric. L1489 IRS is evidence of that this is not always the case. Envelopes may be elongated, asymmetric, warped, and the same is true for the disks. The angular momentum of disk and envelope may not be well aligned either. These asymmetries are likely caused by stellar binarity and interactions with the local environment, such as neighboring clouds and outflows from other protostars.
- As angular resolution is improved by bigger and better telescopes, structural details in young stellar objects are revealed, which cannot be modeled with existing two dimensional radiation transfer codes. However, alongside the development of flexible high dimensional radiation transfer codes, physical models need to be improved as well in order to describe these details.

References

- Adams, F. C., Lada, C. J., & Shu, F. H. 1987, *ApJ*, 312, 788
- Allen, L. E., Calvet, N., D'Alessio, P., et al. 2004, *ApJS*, 154, 363
- André, P. & Montmerle, T. 1994, *ApJ*, 420, 837
- André, P., Ward-Thompson, D., & Barsony, M. 1993, *ApJ*, 406, 122
- Benson, P. J. & Myers, P. C. 1989, *ApJS*, 71, 89
- Bodenheimer, P. 1981, in *IAU Symposium, Vol. 93, Fundamental Problems in the Theory of Stellar Evolution*, ed. D. Sugimoto, D. Q. Lamb, & D. N. Schramm, 5–24
- Boss, A. P. 1993, *ApJ*, 417, 351
- Burkert, A., Bate, M. R., & Bodenheimer, P. 1997, *MNRAS*, 289, 497
- Cassen, P. & Moosman, A. 1981, *Icarus*, 48, 353
- Charnley, S. B., Tielens, A. G. G. M., & Millar, T. J. 1992, *ApJ*, 399, L71
- Goodman, A. A., Benson, P. J., Fuller, G. A., & Myers, P. C. 1993, *ApJ*, 406, 528
- Hogerheijde, M. R. & van der Tak, F. F. S. 2000, *A&A*, 362, 697
- Jørgensen, J. K., Schöier, F. L., & van Dishoeck, E. F. 2004, *A&A*, 416, 603
- Lada, C. J. & Wilking, B. A. 1984, *ApJ*, 287, 610
- Lin, D. N. C. & Pringle, J. E. 1990, *ApJ*, 358, 515
- Luhman, K. L., Allen, L. E., Allen, P. R., et al. 2008, *ApJ*, 675, 1375
- Ritzerveld, J. & Icke, V. 2006, *Phys. Rev. E*, 74, 026704
- Shu, F. H. 1977, *ApJ*, 214, 488
- Terebey, S., Shu, F. H., & Cassen, P. 1984, *ApJ*, 286, 529
- Yorke, H. W. & Bodenheimer, P. 1999, *ApJ*, 525, 330
- Zhou, S. & Evans, II, N. J. 1994, in *Astronomical Society of the Pacific Conference Series, Vol. 65, Clouds, Cores, and Low Mass Stars*, ed. D. P. Clemens & R. Barvainis, 183

